The effect of direct simulated solar irradiation on the thermal and optical behavior of the cellular glass coated with WO_3-based painting

Stefan Danica Novaconi[1], Florina Stefania Rus[1], Madalina Ivanovici[1,2,a)]

[1]National Institute for Research and Development in Electrochemistry and Condensed Matter, Aurel Paunescu Podeanu Street, No. 144, 300569 Timisoara, Romania

[2]Politehnica University of Timisoara, Piata Victoriei, No. 2, 300006 Timisoara, Romania

[a)] Corresponding author: ivanovicigabriela11@yahoo.com

Abstract. In this work, thermal and optical properties were investigated for a commercial glass foam covered with a coating designed for exterior and environmental applications. Hence, a new coating was prepared using WO_3 - a photocatalytic material - as a pigment and acrylic resin - as binder. The thermal properties were studied by monitoring the variation of the temperature at the surface and in different points of the glass foam under controlled operating conditions during exposure to direct simulated solar light. Physical and chemical characterization - RGB and reflectance measurements were conducted for glass foam surface before and after being covered with WO_3-based coating and FT-IR, Raman and EDAX spectroscopy, X-ray diffraction and 3D laser scanning microscopy were used for the as-prepared WO_3 powder, the glass foam and the applied layers of WO_3-based coating. The temperature values reached a plateau after 20 minutes and the calculated heat transfer through the glass foam based on the experimental results was around 106 mW. Photochromism was attributed to the analyzed coating, phenomenon correlated with the optical characteristics of the coating and structural properties of the WO_3 powder. Surface roughness, color, spectral reflectance were improved after multiple layers of the coating.

Keywords: WO_3 pigment, color change, glass foam, direct simulated solar irradiation, spectral reflectance

1. Introduction

Glass foam belongs to new generation materials, designed, among other application, especially as a heat insulator in the building industry. Furthermore, it is considered an ecological and efficient insulation material given the fact that it is being developed both commercially and in the research field from glass waste resources presenting

multiple properties of interest (chemical, physical and biological stability, excellent insulating properties, light weight, fire and water resistance, etc.).

Based on its properties and commercial applications, glass foam, also known as cellular glass, can be used as an insulator for roofs, building facades, sub-base (gravel) and industrial piping and installation. Among the chemical and physical properties intensively studied, there may be mentioned porosity, thermal conductivity, density, sound insulating properties, thermal resistance, compressive strength. Still, limited studies have involved thermal investigation of the glass foam related to heat transfer by conduction or radiation [1–4].

Also, in the context of the necessity of developing smart systems in the construction field as a research trend related to air pollution reduction is to be mentioned the application of exterior photocatalytic coatings that involves the use of photocatalytic compounds as pigments. As reported in the literature, paints using titanium oxide and zinc oxide as pigments due to their photocatalytic properties were studied as potential coatings for reducing air pollutants such as nitrogen oxides and volatile organic compounds from the atmosphere [5, 6]. As well, WO_3 – a visible-light active photocatalytic material was reported to be used as pigment in ceramics, for cosmetic products and for nanoinks. The properties of tungsten trioxide (catalytic, photocatalytic, chromophoric, semiconductor properties) make it appealing for fields such as photocatalysis dedicated to pollution reduction or energy production, sensors, electrochromic and photochromic smart windows [7–9].

In this study, commercial glass foam covered with water-based coating prepared using WO_3 as a pigment was investigated as an environmentally friendly insulation system manifesting multiple properties. The study comprises the evaluation of thermal behavior of the uncovered and covered glass foam with WO_3-based painting as a response to simulated solar radiation exposure in specific conditions in correlation with optical and morphological properties of the commercial glass foam and of the WO_3-based coating. To the best of our knowledge, no studies were reported for preparation and optical characterization of as described WO_3-based painting.

2. Experimental part

2.1. The preparation of the WO_3-based coating

The WO_3 – based coating was prepared using three main components: WO_3 as a pigment – a material largely studied for its photocatalytic activity in the visible-light spectrum, chemical stability, earth abundance and its potential use in the environmental applications, acrylic resin as binder suitable for both interior and exterior finishing coatings, known

for good oxidative, UV stability, resistant to breakage and high temperature, elasticity and widely used for the preparation of emulsion paints and water as a solvent – a cheap, abundant and nontoxic resource [8–10]. The weight ratio of acrylic resin to pigment is 1:1 (each counting for 35 wt%) and the water was adjusted so that the coating can be easily applied by brushing.

The WO_3 pigment was obtained from tungstic acid (pure H_2WO_4 procured from Riedel-de Haën AG) by thermal treatment. The tungstic acid was heated at 600°C for 6 h in air atmosphere, in which the dehydration process occurred so that internal water molecules of the tungstic acid were removed, as presented in equation (1) [11].

$$H_2WO_4 \rightarrow WO_3 + H_2O \quad (1)$$

2.2. FT-IR, Raman, EDAX spectroscopy and X-Ray Diffraction

FT-IR and Raman spectroscopy was used as characterization techniques for the commercial glass foam and synthesized WO_3 powder to identify the main functional groups of their chemical composition. Moreover, to provide a more detailed investigation about chemical composition of the commercial glass foam, EDAX spectroscopy was selected for elemental analysis. FT-IR characterization was performed using FT-IR spectrometer Vertex 70 (Bruker, Germany) using the KBr pellet method in the wavenumber range of 400-4000 cm^{-1} cm^{-1}, 128 scans and a resolution of 8 cm^{-1}. Raman spectra were obtained using a scanning probe microscopy system: Multi Probe Imaging –MultiView 1000TM system (Nanonics Imaging, Israel) and the crystalline phase of the WO_3 powder was investigated using PANalyticalX'Pert Pro MPD-type diffractometer with Cu-Kα radiation (λCu =1.54060 Å) and a 2θ-step of 0.016, from 20° to 80°. Elemental mapping of the commercial glass foam was accomplished using Inspect S PANalytical SEM/EDX.

2.3. Optical characterization and surface morphology investigation of the glass foam and applied WO_3-based coating

Optical properties (RGB and spectral reflectance) were investigated for the glass foam and of the WO_3-based coating applied on the glass foam. The reflectance and RGB measurements provide additional information regarding the color stability of the coating and the changes of the optical response influenced by application of multiple layers.

The RGB measurements consisted of monitoring the proportion of each primary color (red, green and blue), which allows to simulate the color of the investigated surfaces. The color analyses were conducted (with a color Meter-PCE-RGB 2 from PCE Instruments UK Ltd) on the uncovered glass foam and on the coating layers applied on the glass foam before and after the system was exposed to the direct simulated solar light.

The reflectance was measured on the uncoated glass foam and on the applied layers of the coating before the thermal experiments. The reflectance analysis was accomplished by an integrating sphere of 50 mm (model ISP-50-8-R-GT from Ocean Optics) connected to the Jaz modular UV-VIS spectrophotometer (procured from Ocean Optics) and the light source (LS-1 from Ocean Optics).

The surface texture of the layers of WO_3-based coating was analyzed in comparison with the uncoated glass foam using 3D laser scanning microscopy. Therefore, the images of the surfaces were obtained using 3D laser scanning microscope OLS 4000 Lext Olympus.

2.4. Thermal investigation

The thermal properties of the glass foam covered with WO_3-based coating system were analyzed by simulating real conditions for which this system can be used as an external insulating layer of the building envelope. The commercial glass foam, Pinosklo cellular glass, was cut into pieces of the following sizes: 10 cm × 10 cm × 4 cm (length × depth × height) and subjected to the experimental investigations. Each piece was fixed in a polystyrene box so that the heat transfer between the exterior and interior does not occur on the sideways. The upper surface of the samples was exposed to the heating source - simulated solar radiation (provided by Sol2A 94042A, Oriel Instruments/Newport Corporation) and the bottom surface is placed on a stainless-steel surface. The ambient temperature was maintained constant at 23°C.

For two hours, the temperature was measured at the surface of the sample with infrared camera (Fluke Ti110 thermal imaging camera) and in certain points inside the sample situated at equal distances across the sample height using type K thermocouples connected to a thermometer with 4 channels (model TM –946 from Lutron Electronic). The temperature measurements were conducted for glass foam sample before and after applying each layer of WO_3 - based coating. Four layers of WO_3–based coating were applied on the glass foam and the irradiance of the simulated solar radiation at the surface of the sample was around 895 W/m^2 in the visible domain and 10 W/m^2 for UV domain.

3. Results and discussion

3.1. Spectroscopic characterization of WO_3 powder used as pigment and of the commercial glass foam

The FT-IR spectra (figure 1 (a)) of the WO_3 powder reveals two peaks associated with the adsorbed water molecules at ~3459 cm^{-1} and ~1640 cm^{-1} ascribed to stretching vibration – ν(O-H) and, respectively, to the bending vibration mode δ(H–O–H). The broad peak situated at 840 cm^{-1} can be attributed to the ν(W-O-W) vibration with a shoulder

present at 776 cm^{-1} which can be assigned to the ν(O-W-O) vibrations [12, 13]. Additional vibrational modes are identified in the Raman spectra (figure 1 (b)) between 50 cm^{-1} and 1000 cm^{-1} at 720, 812, 332 and 278 cm^{-1}. As reported in the study [14], the revealed bands of the WO_3 raman spectra correspond to the crystalline monoclinic tungsten trioxide (*m*-WO_3).

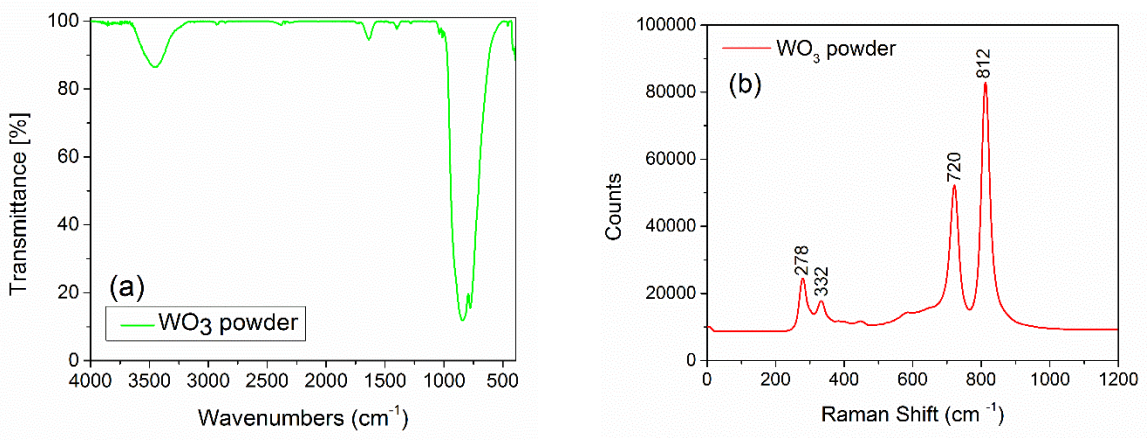

Figure 1. FT-IR spectra (a) and Raman spectra (b) of the WO_3 powder

Therefore, the peaks found at 720 cm^{-1} and 812 cm^{-1} are ascribed to the stretching vibration mode (ν(O-W-O)) and the peaks situated at 278 cm^{-1} and respectively 332 cm^{-1} can be attributed to the bending vibration mode O-W-O of bridging oxygen [12–14].

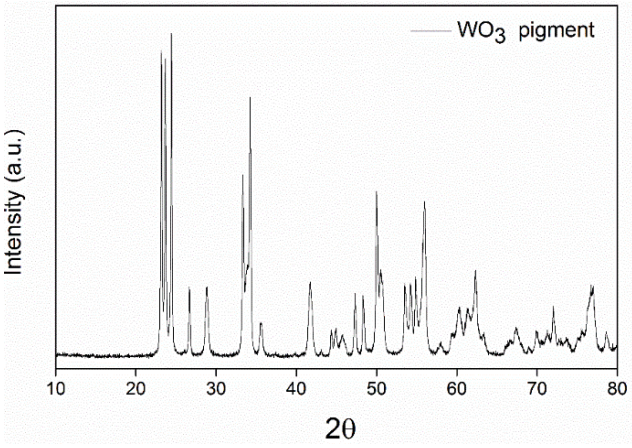

Figure 2. Powder XRD diagram of WO_3 pigment

The purity and crystalline phase of the synthesized WO_3 were further investigated using X-ray diffraction spectroscopy. The XRD pattern (figure 2) shows diffraction peaks that are ascribed entirely 100% to the monoclinic

crystalline structure of WO_3 with the lattice parameters of a = b = c = 5.078 Å as confirmed by the standard card (JCPDS: 75–2072) using Rietveld refinement analysis, reflecting the high purity of the crystalline phase

Based on the information provided by XRD analysis the structural parameters of the WO_3 powder are presented in table 1. The sharp peaks at 2θ = 23.18, 23.63, 24.38, 26.7, 28.94, 33.38, 34.26, 35.44, 41.74, 47.27, 48.25, 49.99, 53.46, 54.23, 54.88, 55.95, 76.8 correspond to the planes (002), (020), (202), (120), (112), (021), (202), (220), (221), (002), (040), (400), (022),(202), (240), (401), (422) [15, 16].

Table 1. Structural parameters of WO_3 powder

Formula $W_{6,00}O_{2,00}$	a [Å] - 5,078(2)
100% WO_3	b [Å] - 5,078(2)
Spatial group P m –3 n (223)	c [Å] - 5,078(2)
The molar mass [g/mol]- 1135,0990	α [degree] - 90
Calculated density [g/cm^3] - 14,3895	β [degree] - 90
V (10^6 pm^3) - 130,97100	γ [degree] - 90

As widely studied, it has to be mentioned that the properties of WO_3, including but not limited to crystal phase, surface chemistry, the band gap, that are likewise interdependent properties, have a strong impact further in their application, such as photocatalysis, chromism and semiconductivity [8, 9]. In the study [9], it has been pointed out that WO_3 powders of different crystal phases (m-WO_3, h-WO_3, o-$WO_3 \cdot 0.33H_2O$ and its combinations) and morphologies (nanorods, cuboidal nanoplates, nanowires, etc.) led to different values of band gaps and also distinct appearance (yellow or blue color). The variations of WO_3 powder structural and morphological properties involved also different photocatalytic performances. In other experimental studies [17, 18] it has been reported that enhanced photocatalytic activity was obtained for m-WO_3 when compared to h-WO_3 and, respectively, for o-WO_3/Al-W when compared to c-WO_3/Al-W. Similarly, it was illustrated that photochromic activity is affected by the crystal phase of WO_3 therefore, hexagonal phase of WO_3 showed better photochromic properties than cubic phase [19].

Similar to the FT-IR spectrum of WO_3, in the FT-IR spectra of the glass foam (figure 3 (a)), the bands from 3448 cm^{-1} and 1625 cm^{-1} correspond to the vibrations of water groups. As it is specified on the producer site, the

commercial glass is produced from recycled materials (such as container and window glass), whereas the carbon black is used as foaming agent. Most common glasses used for production of containers and windows are soda-lime glass and potash glass. The main constituent oxides of these types of glasses are SiO_2, CaO, Na_2O, K_2O, of which SiO_2 represents the major component (>50%-wt%) [20–22].

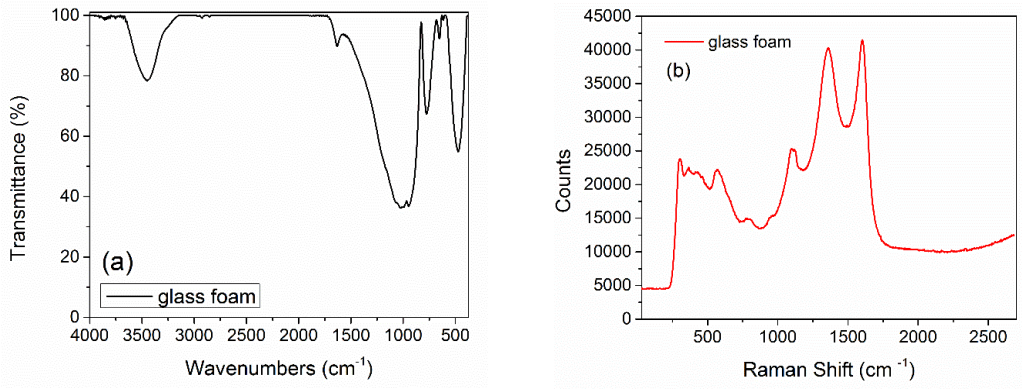

Figure 3. FT-IR (a) and Raman (b) spectra of the commercial glass foam

The peaks revealed in the FT-IR spectra of the commercial glass foam correspond to the vibrations of SiO_2 as further presented: the broad band at 1022 cm^{-1} may be ascribed to the Si–O–Si anti–symmetric stretching of bridging oxygen within the tetrahedral and the weak peak at 920–980 cm^{-1} can be ascribed to Si–O– stretching with non-bridging oxygens. The band at 770 cm^{-1} and 475 cm^{-1} can be attributed to the Si–O–Si symmetric stretching vibrations of bridging oxygens and to the bending modes of Si–O–Si or O–Si–O, respectively [23].

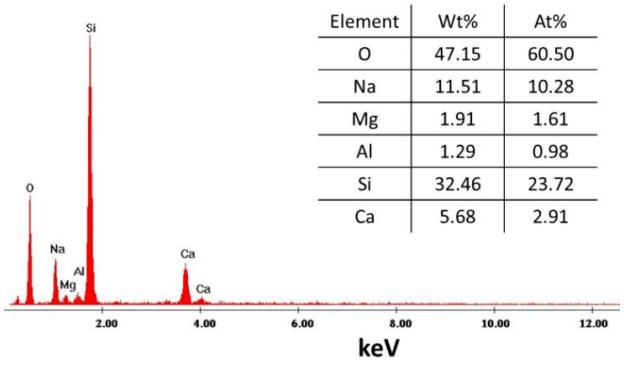

Element	Wt%	At%
O	47.15	60.50
Na	11.51	10.28
Mg	1.91	1.61
Al	1.29	0.98
Si	32.46	23.72
Ca	5.68	2.91

Figure 4. EDAX elemental analysis of the commercial glass foam

In the Raman spectra (figure 3(b)) of the glass foam, two intense bands are observed at 1606 cm^{-1} and 1359 cm^{-1} that correspond to the carbon element used as foaming agent, explaining the black color of the glass foam. Also, the peak

at 1107 cm^{-1} is characteristic of silica tetrahedra with one non-bridging oxygens. The bands between 300 cm^{-1} and 600 cm^{-1} are very likely to correspond to vibration of oxygen atoms in Si-O bonds but can also be attributed to M-O-M groups, where M can represent Si or other elements [24, 25]. Based on the EDAX analysis, the investigation of the elemental composition for commercial glass foam is more detailed via semi-quantitative analysis. EDAX spectra (figure 4) attests the oxygen as the major element followed by silicon given by the silicon dioxide - the main component of the glass foam, as previously mentioned. The other elements revealed here are Na (11.51 wt%), Ca (5.68 wt%), Mg (1.91 wt%) and Al (1.29 wt%).

3.2. Optical characterization and surface morphology investigation of the glass foam and WO_3-based coating

The optical properties in terms of spectral reflectance (diffuse reflection) and color, investigated using the RGB model, were evaluated for the uncovered glass foam sample in comparison with the glass foam sample after applying every layer of the WO_3- based coating.

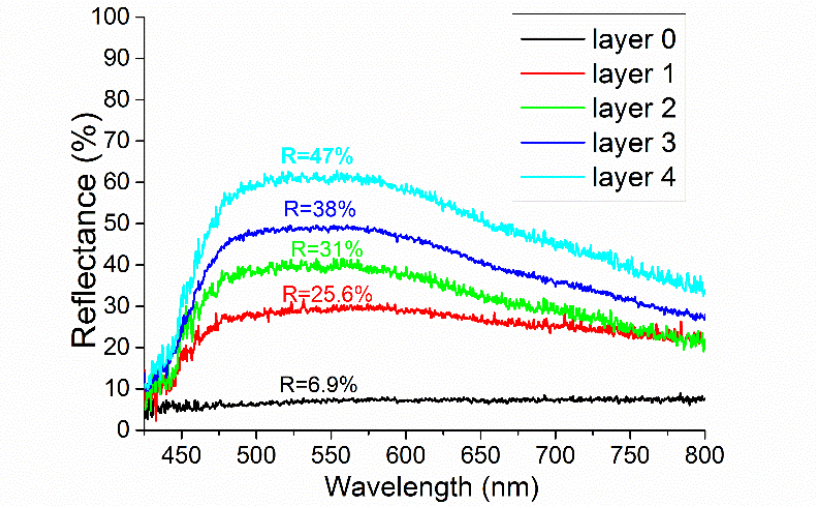

Figure 5. The reflectance of layer 1, layer 2, layer 3 and layer 4 of WO_3-based coating applied on the glass foam compared to glass foam with no coating applied (layer 0)

As presented in figure 5, the reflectance curve indicates that the maximum reflectance values for layers 1–4 was found in the wavelength range of 480÷580 nm. This domain corresponds mainly to green wavelength spectrum and to wavelength spectrum that is attributed to cyan and yellow [26]. The reflectance curve for the uncoated glass foam is nearly uniform across the spectrum between 400 and 700 nm, which suggests the dark grey of the glass foam. The

reflection increases from 25.6% to 47% for layers 1−4, indicating a more intense color of the coating and a more proper covering of the coating on the glass foam.

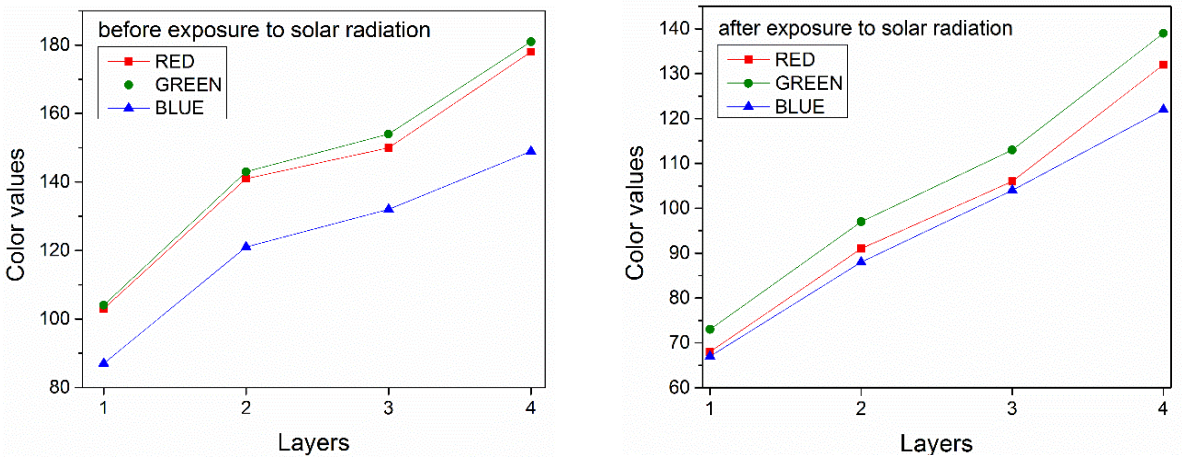

(a) (b)

Figure 6. Modification of RGB values (expressed from 0 to 255) for each layer of applied WO_3-coating (a) before and (b) after exposure to simulated solar light

Still, the color of the coatings showed significant changes after being exposed to simulated solar radiation (figure 6). The color change after exposure to simulated light, expressed by the RGB model, is indicated by the decrease of R, G, B values with approximately 30–40 units for each layer applied, which results in a decrease strength of the color. Moreover, the green-yellow color, more clearly revealed for layer 4, as illustrated in figure 7, turns into a green bluish color. This information is also revealed by comparing the proportion of each primary color before and after exposure to simulated solar light. Before irradiation, values attributed to R and G are almost equal and the proportion of B is lower compared to R and G. After irradiation, the proportion of R decreases in comparison with G, being very similar to B and the proportion of B in relation to G increases comparing to results obtained before irradiation.

The color change of the coating could be explained by photochromic properties of the WO_3, as reported in scientific literature. Considering the conduction properties of the WO_3, electrons (e^-) and holes (h^+) pairs are generated due to light irradiation. The former enter the conduction band of WO_3 and the holes react with water from the system forming H_xWO_3 (equation 2), resulting in a color change. The change of color can vary from yellow to blue [8, 19].

$$WO_3 + xH^+ + xe^- \rightarrow H_xWO_3 \quad (2)$$

As previously mentioned, WO_3 is a well-known semiconductor with a large applicability spectrum for which the color is depending on the oxidation state of the tungsten atoms in the crystal structure. Therefore, the capacity of the powder capturing photons, that is, the amount of photon induced electron–hole pairs directly influence the photochromic properties of the WO_3 compound [8, 19].

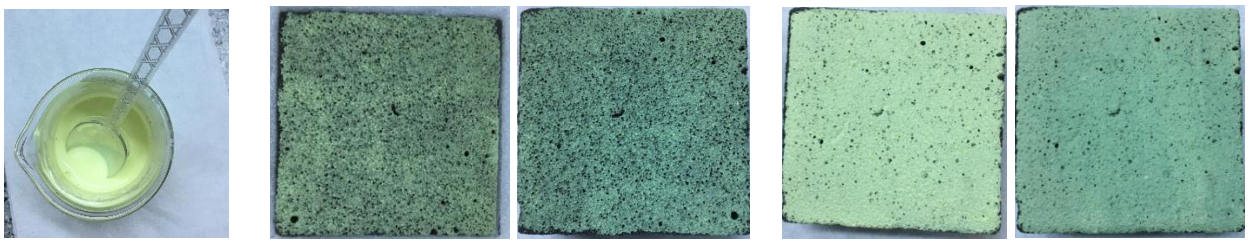

WO_3-based coating | Before irradiation | after irradiation | before irradiation | after irradiation

Layer 1 | Layer 4

Figure 7. The photos of WO_3-based coating (left side) and of the glass foam covered with of WO_3-based coating (layer 1 and layer 4) before and after solar irradiation

The glass foam has a porous structure and for this reason multiple layers of the coating were required to achieve o good coverage. Four layers, as previously mentioned, were involved in the study.

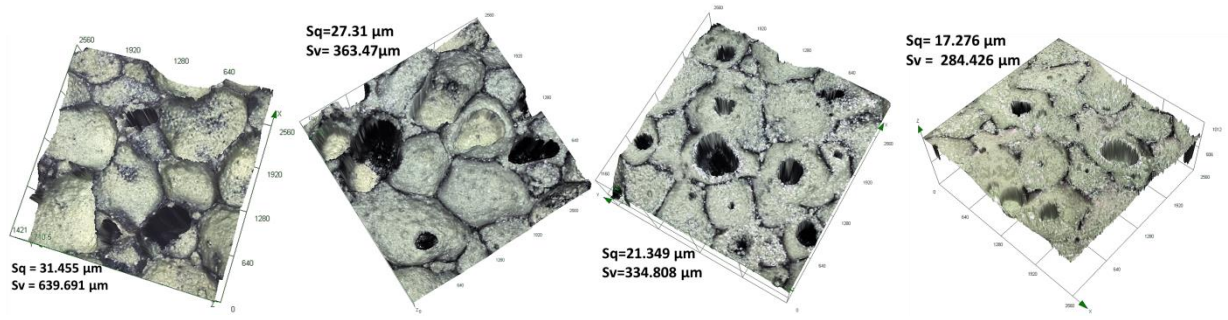

(a) (b) (c) (d)

Figure 8. 3D images for the porous surface of the glass foam covered with (a) layer 1, (b) layer 2, (c) layer 3 and (d) layer 4 of WO_3-based coating

In figure 8, it is shown that a more homogeneous dispersion of the coating is achieved as the number of layers increases, which led to the decrease of surface roughness (Sq) from 31.45 µm to 17.28 µm and to the decrease of maximum valley depth (Sv) from 640 µm to 285 µm based on the 3D images.

3.3. Thermal behavior evaluation of the glass foam

In figure 9, it is presented the thermal behavior of the glass foam sample before and after being covered with WO_3-based coating obtained under specific experimental conditions: exposure to simulated solar radiation and constant ambient temperature.

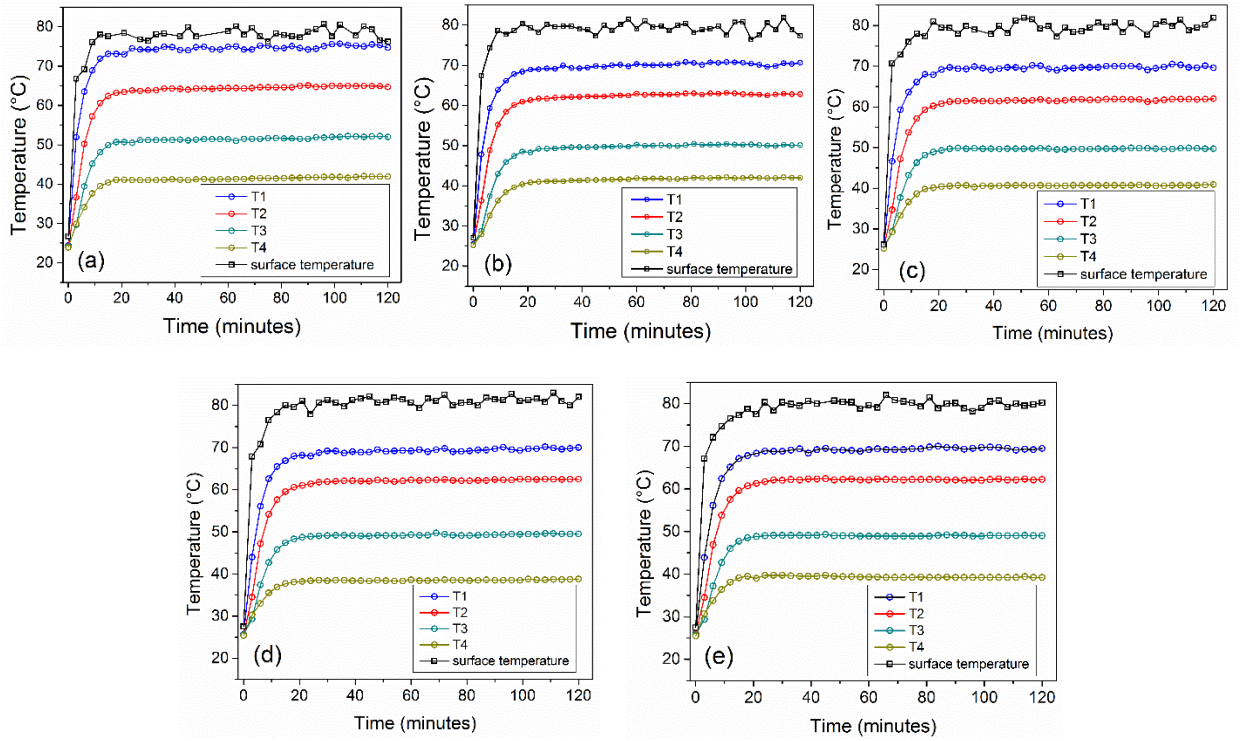

Figure 9. Thermal response of the uncoated glass foam (a) and of the glass foam covered with WO_3-based coating ((b) – layer 1; (c) – layer 2; (d) – layer 3; (e) – layer 4)) during the exposure to simulated solar radiation

Therefore, in the first step, when no coating was applied, it can be noticed that during the radiation exposure, the temperature of the surface (Tsupr) and the temperature measured at the four points across the glass foam sample height (T1, T2, T3, T4) increased rapidly from approximately 27°C and respectively 24°C (for T1, T2, T3, T4) to ~ 78–80°C and respectively 74°C, 64°C, 51°C, 41°C after 20 min, followed by temperature stabilization specified by a plateau value in the range between 20 and 120 minutes for all five monitored zones.

The temperature values inside the glass foam sample decreased constantly from one measuring zone to the following one as the heat of the solar radiation passed through across the height of the sample, for which the internal heat conduction through the glass foam sample was around 106 mW. The internal heat flux was calculated with Fourier's

law heat conduction equation based on the experimentally investigated temperatures across the glass foam thickness after the temperature plateau values were achieved [27].

Very similar trends of the temperature change over time were achieved after applying each layer of WO_3-based coating, indicating that the coating does not influence the thermal response of the glass foam. This can be explained based on the assumption that the extent of the optical response (in terms of reflected radiation) and the emissivity of the coating layering is insignificant to lead to a temperature modification considering the involved experimental conditions.

When it comes to thermal insulating properties of glass foam, it was pointed out, according with other experimental studies concerning the synthesis of glass foam from glass waste and to obtain valuable properties of interest, that the thermal conductivity depends on the porosity and compressive strength determined by the type of foaming agent, the raw materials and the synthesis conditions used for the glass foam production [2, 28–30].

4. Conclusion

Based on the optical investigation of the glass foam and of the applied layers of the WO_3-based coating, spectral reflectance of the coating increased from the 6.9% to 47% with the number of applied layers in the range between 480 and 580 nm corresponding to the yellow-green color, as visually detected. Moreover, the color change after solar irradiation given by photochromic properties of the WO_3 can be considered an indicator of photon induced electron–hole pairs mechanism that precede also the photocatalysis phenomenon. Still, supplementary studies are undisputable needed for investigating the photocatalytic properties of the coating to develop efficient coatings for pollutant reduction.

Considering direct simulated solar irradiation, the surface temperature and the temperature inside the glass foam reached approximately 80°C and respectively 74°C, 64°C, 51°C, 41°C (for T1, T2, T3, T4) with no modification after application of the WO_3-based coating on the glass foam.

As the glass foam is a porous material, the 3D scanning images illustrated that a more proper application of the WO_3 based coating was obtained after multiple layers, emphasized by the decrease of surface roughness. The FT-IR, Raman and XRD spectra led to the identification of the main functional groups of the commercial glass foam, especially Si-O and Si-O-Si and carbon and of the monoclinic crystalline phase of the synthesized WO_3 pigment. EDAX spectra identified other elements of the glass foam such as Na, Ca, Mg and Al.

Acknowledgment

This work was sustained within the project PN-III-P1-1.2-PCCDI-2017-0391/CIA_CLIM-Smart buildings adaptable to the climate change effects granted by Romanian Minister of Research and Innovation, CCCDI–UEFISCDI.

References

[1] Y.I. Vaisman, A.A. Ketov, P.A. Ketov, The scientific and technological aspects of foam glass production, Glass Physics and Chemistry 41 (2015) 157–162. https://doi.org/10.1134/S1087659615020133

[2] Y. Liu, J. Xie, P. Hao, Y. Shi, Y. Xu, X.Ding, Study on factors affecting properties of foam glass made from waste glass, Journal of Renewable Materials 9(2) (2021) 237-253. http://doi.org/10.32604/jrm.2021.012228

[3] J. Lu, K. Onitsuka, Construction utilization of foamed waste glass, Journal of Environmental Sciences (China) 16(2) (2004) 302-307.

[4] M.J. Varady, A.G. Fedorov, Combined radiation and conduction in glass foams, Journal of Heat Transfer – transactions of The Asme 124(6) (2002) 1103–1109. https://doi.org/10.1115/1.1513579

[5] B.A. van Driel, S.R. van der Meer, K.J. van den Berg, J. Dik, Determining the presence of photocatalytic titanium white pigments via embedded paint sample staining: a proof of principle, Studies in Conservation 64(5) (2018) 261-272. https://doi.org/10.1080/00393630.2018.1503863

[6] D. Truffier-Boutry, B. Fiorentino, V. Bartolomei, R. Soulas, O. Sicardy, et al., Characterization of photocatalytic paints: a relationship between the photocatalytic properties – release of nanoparticles and volatile organic compounds, Environmental science: Nano 4(10) (2017) 1998 – 2009. http://doi.org/10.1039/c7en00467b

[7] P. Patnaik, Handbook of Inorganic Chemical Compounds, McGraw-Hill, Burlington, 2003.

[8] S. Wang, W. Fan, Z. Liu, A. Yu, X. Jiang, Advances on tungsten oxide based photochromic materials: strategies to improve their photochromic properties, Journal of Materials Chemistry C 6(2) (2018) 191-212. http://doi.org/10.1039/C7TC04189F

[9] D. Nagy, D. Nagy, I.M. Szilágyi, X. Fan, Effect of the morphology and phases of WO_3 nanocrystals on their photocatalytic efficiency, RSC Advances 6(40) (2016) 33743-33754. http://doi.org/10.1039/C5RA26582G

[10] Á. Serrano-Aroca, Acrylate Polymers for Advanced Applications, IntechOpen, 2020. http://doi.org/10.5772/intechopen.77563

[11] H.I.S. Nogueira, A.M.V. Cavaleiro, J. Rocha, T. Trindade, J.D. Pedrosa de Jesus, Synthesis and characterization of tungsten trioxide powders prepared from tungstic acids, Materials Research Bulletin 39(4-5) (2004) 683–693. https://doi.org/10.1016/j.materresbull.2003.11.004

[12] N. Prabhu, S. Agilan, N. Muthukumarasamy, C.K. Senthilkumaran, Effect of temperature on the structural and optical properties of WO_3 nanoparticles prepared by solvo thermal method, Digest Journal of Nanomaterials and Biostructures 8(4) (2013) 1483-1490.

[13] M. Gotic´, M. Ivanda, S. Popovic´, S. Music´, Synthesis of tungsten trioxide hydrates and their structural properties, Materials Science and Engineering: B 77(2) (2000) 193-201. https://doi.org/10.1016/S0921-5107(00)00488-8

[14] M.F. Daniel, B. Desbat, J.C. Lassegues, B. Gerand, M. Fjglarz, Infrared and raman study of WO_3 tungsten trioxides and WO_3, xH_2O tungsten trioxide hydrates, Journal of Solid State Chemistry 67 (1987) 235-247. https://doi.org/10.1016/0022-4596(87)90359-8

[15] J. Rajeswari, P. Kishore, B. Viswanathan, T.K. Varadarajan, Facile hydrogen evolution reaction on WO_3 nanorods, Nanoscale Research Letters 2 (2007) 496-503. https://doi.org/10.1007/s11671-007-9088-y

[16] M. Raja, J. Chandrasekaran, M. Balaji, The structural, optical and electrical properties of spin coated WO_3 thin films using organic acids, Silicon 9 (2017) 201–210. https://doi.org/10.1007/s12633-016-9413-0

[17] I.M. Szilágyi, B. Fórizs, O. Rosseler, Á. Szegedi, P. Németh, Péter Király, G. Tárkányi, B. Vajna, K. Varga-Josepovits, K. László, A.L. Tóth, P. Baranyai, M. Leskelä, WO_3 photocatalysts: Influence of structure and composition, Journal of Catalysis 294 (2012) 119-127. https://doi.org/10.1016/j.jcat.2012.07.013

[18] S. Higashino, M. Miyake, T. Ikenoue, T. Hirato, Formation of a photocatalytic WO_3 surface layer on electrodeposited Al–W alloy coatings by selective dissolution and heat treatment, Scientific Reports 9(1) (2019) 16008. https://doi.org/10.1038/s41598-019-52178-6

[19] R. Huang, Y. Shen, L. Zhao, M. Yan, Effect of hydrothermal temperature on structure and photochromic properties of WO_3 powder, Advanced Powder Technology 23(2) (2012) 211-214. https://doi.org/10.1016/j.apt.2011.02.009

[20] V.W. Francis Thoo, N. Zainuddin, K.A. Matori, S.A. Abdullah, Studies on the potential of waste soda lime silica glass in glass ionomer cement production, Advances in Materials Science and Engineering (2013). https://doi.org/10.1155/2013/395012

[21] M. Vilarigues, R.C. da Silva, Characterization of potash-glass corrosion in aqueous solution by ion beam and IR spectroscopy, Journal of Non-Crystalline Solids 352(50-51) (2006) 5368-5375. https://doi.org/10.1016/j.jnoncrysol.2006.08.032

[22] W.B. Stern, Y. Gerber, Potassium–calcium glass: new data and experiments, Archaeometry 46(1) (2004) 137-156. https://doi.org/10.1111/j.1475-4754.2004.00149.x

[23] H.A. ElBatal, M.Y. Hassaan, M.A. Fanny, M.Y. Hassaan, Optical and FT infrared absorption spectra of soda lime silicate glasses containing nano Fe_2O_3 and effects of gamma irradiation, Silicon 9 (2017) 511–517. https://doi.org/10.1007/s12633-014-9262-7

[24] L. Bokobza, J.-L. Bruneel, M. Couzi, Raman spectra of carbon-based materials (from graphite to carbon black) and of some silicone composites, C – Journal of Carbon Research 1(1) (2015) 77-94. https://doi.org/10.3390/c1010077

[25] A.K. Yadav, P. Singh, A review of the structures of oxide glasses by Raman spectroscopy, RSC Advances 5(83) (2015) 67583-67609. https://doi.org/10.1039/C5RA13043C

[26] S. Bhowmick, The RGB rendering of visible wavelength lights (2019 02 28 14 47 31 UTC) 2017. 10.13140/RG.2.2.14324.71040

[27] C. H. Forsberg, Chapter 1 - Introduction to heat transfer, in C. H. Forsberg (Eds.) Heat Transfer Principles and Applications, Academic Press, 2020, pp. 1-21. https://doi.org/10.1016/B978-0-12-802296-2.00001-9

[28] E. Kim, K. Kim, O. Song, Properties of foamed glass upon addition of nanocarbon and sintering temperatures, Journal of Asian Ceramic Societies 8 (2020) 123-129. https://doi.org/10.1080/21870764.2020.1712798

[29] Z. Qin, G. Li, Y. Tian, Y. Ma, P. Shen, Numerical simulation of thermal conductivity of foam glass based on the steady-state method, Materials (Basel) 12(1) (2018) 54. https://doi.org/10.3390/ma12010054

[30] N.S. Karandashova, B.M. Goltsman, E.A. Yatsenko, Analysis of influence of foaming mixture components on structure and properties of foam glass, IOP Conference Series: Materials Science and Engineering 262 (2017) 012020. https://doi.org/10.1088/1757-899X/262/1/012020